MAJOR ARTICLE

HIV-1 Infection Accelerates Age According to the Epigenetic Clock

Steve Horvath[1,3] and Andrew J. Levine[2]

[1]Department of Human Genetics, [2]Department of Neurology, David Geffen School of Medicine, and [3]Department of Biostatistics, School of Public Health, University of California–Los Angeles

Background. Infection with human immunodeficiency virus type 1 (HIV) is associated with clinical symptoms of accelerated aging, as evidenced by the increased incidence and diversity of age-related illnesses at relatively young ages and supporting findings of organ and cellular pathologic analyses. But it has been difficult to detect an accelerated aging effect at a molecular level.

Methods. Here, we used an epigenetic biomarker of aging based on host DNA methylation levels to study accelerated aging effects due to HIV infection. DNA from brain and blood tissue was assayed via the Illumina Infinium Methylation 450 K platform.

Results. Using 6 novel DNA methylation data sets, we show that HIV infection leads to an increase in epigenetic age both in brain tissue (7.4 years) and blood (5.2 years). While the observed accelerated aging effects in blood may reflect changes in blood cell composition (notably exhausted cytotoxic T cells), it is less clear what explains the observed accelerated aging effects in brain tissue.

Conclusions. Overall, our results demonstrate that the epigenetic clock is a useful biomarker for detecting accelerated aging effects due to HIV infection. This tool can be used to accurately determine the extent of age acceleration in individual tissues and cells.

Keywords. HIV-1; DNA methylation; epigenetics; aging; biomarker.

While antiretroviral therapy for human immunodeficiency virus (HIV) infection is highly effective at preventing AIDS-related complications, treated patients are at a significant risk for a number of diseases typically associated with older age, including cardiovascular disease, osteoporosis, cancer, neurocognitive impairment, and frailty [1–11]. Among the aging HIV-infected population, it has become evident that the incidence of HIV-associated non–AIDS-defining conditions is increasing [12]. In recent years, the Working Group on HIV and Aging published a report for the National Institutes of Health Office of AIDS Research, in which it stated that the cause of this increasing incidence is unclear but proposed that it may be due to an accelerated aging process [13]. To show that HIV infection is associated with accelerated normal aging, one first needs to understand what is meant by normal aging and to find a way of measuring it. Owing to its modest accuracy, telomere length will probably have to be supplemented by additional biomarkers of aging when it comes to understanding and measuring normal aging. DNA methylation levels are particularly promising biomarkers of aging since chronological age (ie, the calendar years that have passed since birth) has a profound effect on DNA methylation levels in most human tissues and cell types [14–23]. Several recent studies support measuring accelerated aging effects by using DNA methylation levels [24, 25]. The noteworthy aspect of our recently developed epigenetic clock (based on 353 dinucleotide markers known as cytosine phosphate guanines [CpGs]) is its broad applicability to most human cell types, tissues, and organs [25]. Predicted age, referred to as DNA methylation age, correlates with chronological age in sorted cell types ($CD4^+$ T cells, monocytes, B cells, glial cells, and neurons) and

Received 21 October 2014; accepted 5 May 2015; electronically published 12 May 2015.

Correspondence: Steve Horvath, PhD, Department of Human Genetics, Gonda Research Center, UCLA, 695 Charles E. Young Dr S, Box 708822, Los Angeles, CA 90095-7088 (shorvath@mednet.ucla.edu).

The Journal of Infectious Diseases® 2015;212:1563–73

DOI: 10.1093/infdis/jiv277

in tissues and organs, including whole blood, brain, breast, kidney, liver, lung, and saliva [25].

The epigenetic clock is an attractive biomarker of aging because (1) it is more strongly correlated with chronological age than previous biomarkers, including telomere length [26,27]; (2) it is prognostic of all-cause mortality in later life [28]; and (3) it correlates with measures of physical and mental fitness in older age [29]. The usefulness of the method has been demonstrated in recent case studies, including one showing that obesity accelerates epigenetic aging in liver tissue [27]. Further, trisomy 21 (Down syndrome) accelerates epigenetic aging in blood and brain tissue [30].

Although HIV infection appears to lower the age at which individuals develop age-related illnesses, it is not yet known whether DNA methylation age is a biologically meaningful biomarker of accelerated aging in the context of HIV infection. Here we use both blood and brain tissue from HIV-infected subjects (hereafter, "cases") and uninfected controls (hereafter, "controls") to show that HIV infection is significantly associated with increased age acceleration according to the epigenetic clock.

MATERIALS AND METHODS

DNA Methylation Data Sets

An overview of the 11 Illumina DNA methylation data sets used in this article is provided in Table 1. We generated 6 novel DNA methylation data sets and used 5 publicly available data sets. Our 6 novel data sets are available from Gene Expression Omnibus super-series GSE67752. Details on the individual data sets can be found in Table 1 and Supplementary 1. The 3 brain data sets came from the National NeuroAIDS Tissue Consortium (NNTC) [31]. Informed consent and all study procedures were approved by the institutional review boards (IRBs) at the 4 individual sites composing the NNTC.

Novel Data Set 1: Various Brain Specimens From Cases and Controls

We generated Illumina Infinium 450 K data from 130 fresh frozen brain samples from 84 different subjects (71 cases and 13 controls). Specifically, we considered specimens from the cerebellum (20 cases and 4 controls), frontal lobe (2 cases and 4 controls), hippocampus (4 controls), medial frontal cortex (18 cases), occipital cortex (59 cases and 13 controls), and temporal cortex (4 controls). For the cases, the median year of death was 2005 (range, 1999–2013). Additional details can be found in Table 2. In total, there were 99 samples from cases and 31 samples from controls of similar ages. DNA methylation data from cases and controls were generated at the same time and randomized across plates and chips. HIV load information was available for blood (in the last specimen obtained prior to death) and cerebrospinal fluid (CSF) specimens.

The protein abundance levels of the IBA1 marker were assessed as follows: 5-μm-thick, formalin-fixed, paraffin-embedded

Table 1. Overview of the DNA Methylation Data Sets

Data Set[a]	DNA Origin	Description	Illumina Platform	Illumina Arrays, No.	HIV-Infected Subjects, No.	Reference	Public Availability[b]
1	Brain tissue	Various brain regions from HIV-infected and uninfected subjects	450 K	130	99	Novel data	GSE59457
2	Brain tissue	Frontal lobe from HIV-infected and uninfected subjects	450 K	33	8	Novel data	GSE67749
3	Brain tissue	Cerebellum from HIV-infected and uninfected subjects	450 K	20	8	Novel data	GSE67748
4	Whole blood	HIV-infected and uninfected subjects	450 K	92	24	Novel data	GSE53841
5	Whole blood	HIV-infected and uninfected subjects	450 K	92	23	Novel data	GSE67751
6	PBMCs	HIV-infected men	450 K	109	109	Novel data	GSE53840
7	Whole blood	Healthy controls	450 K	335	0	Liu et al [37]	GSE42861
8	Blood cell types	4 healthy subjects	27 K	28	0	Accomando et al [39]	GSE39981
9	Blood cell types	6 healthy men	450 K	60	0	Reinius et al [40]	GSE35069
10	$CD4^+$ T cells and monocytes	23 healthy subjects	27 K	46	0	Rakyan et al [10]	GSE20242
11	Blood cell types	6 healthy subjects	450 K	42	0	Zilbauer et al [41]	E–ERAD–179

Abbreviations: HIV, human immunodeficiency virus; PBMC, peripheral blood mononuclear cell.

[a] Illumina data sets used in this article.

[b] Either Gene Expression Omnibus identifier or ArrayExpress identifier.

Table 2. Clinical Characteristics of the Brain Data Set From the National NeuroAIDS Tissue Consortium

Variable	Subjects, No.	Value
Age at death, y	71	45.9 ± 9.1
Infection duration, y	65	13 ± 6.9
Nadir $CD4^+$ T-cell count, cells/mm^3	71	27.7 ± 33.2
Plasma viral load at diagnosis, log_{10} copies/mL	70	3.75 ± 1.35
CSF viral load, log_{10} copies/mL	48	2.75 ± 1.37
$CD4^+$ T-cell count at death, cells/μL	70	114 ± 141
Global neurocognitive clinical rating[a]	71	5.3 ± 2
HIV-related neurocognitive disorder[b]	71	
Taking combined antiretroviral therapy	65	
Neuropathological finding	31	
Alzheimer type 2 gliosis	7	
Aseptic leptomeningitis	4	
Focal infarct	4	
Hemorrhage	2	
HIV encephalitis	8	
Hypoxic/ischemic damage	3	
Microglial nodule encephalitis	9	
Lymphoma	1	
Other noninfectious pathologies	4	
Other infections	2	
Tuberculosis	1	

Data are mean ± SD or percentage (no.) of cases.

Abbreviations: CSF, cerebrospinal fluid; HIV, human immunodeficiency virus.

[a] Global neurocognitive clinical rating was assessed as described elsewhere [32].

[b] HIV-related neurocognitive disorder was assessed as described elsewhere [33, 34].

brain sections were immunostained with mouse monoclonal antibody against Iba-1 (Wako), as previously described [35]. The DAB-stained sections were digitally scanned using a microscopy slide scanner (Aperio ScanScope GL, Leica, Vista, California) equipped with a 20× objective lens (yielding the resolution of 0.5 μm/pixel). Anatomical areas of interest were digitally delineated and the immunoreactivity signals quantified within each of these areas using the Image-Pro Analyzer software (version 6.3; MediaCybernetics, Bethesda, Maryland), as previously described in detail [36].

Novel Data Set 2: Frontal Lobe Specimens From Cases and Controls

Fresh frozen frontal lobe samples from 8 cases and 25 controls were evaluated. The 8 cases had a mean age of 44 years (range, 27–64 years). Years of death ranged from 2000 to 2013. Years of HIV diagnosis ranged from 1989 to 1996. The mean number of years living with HIV (until death) was 12 years (range, 1–19 years).

Novel Data Set 3: Cerebellum Specimens From Cases and Controls

Fresh frozen cerebellar samples from 8 cases and 12 controls were evaluated. The 8 cases correspond to the subjects used in data set 2.

Novel Data Set 4: Blood Specimens From Cases and Controls

Peripheral blood mononuclear cells (PBMCs) isolated from 92 subjects were evaluated. The 24 cases had a mean age of 49 years (range, 29–67 years). The cases were from the National Neurological AIDS Bank study or Multicenter AIDS Cohort Study in Los Angeles. Informed consent and all study procedures were approved by the University of California–Los Angeles Medical IRB. The 68 controls had a mean age of 36 years (range, 18–74 years). The controls were nonmedicated subjects from a previously published study (GSE41169) [19]. DNA methylation data from cases and controls were generated by the same core facility.

Novel Data Set 5: Blood Specimens From Cases and Controls

PBMCs were obtained from the National Neurological AIDS Bank study or Multicenter AIDS Cohort Study in Los Angeles. The 23 cases had a mean age of 45 years (range, 24–68 years). The 69 controls had a mean age of 51 years (range, 35–64 years).

Data Set 6: Adult Male Cases, Novel Data

PBMC samples were obtained from 109 adult male cases to study the relationship between viral load, blood cell counts, and epigenetic age acceleration. This data set did not contain any controls. Cases were from the National Neurological AIDS Bank study or the Multicenter AIDS Cohort Study in Los Angeles. The mean age was 52 years (range, 31–68 years). The following measured blood cell count data were available: mean $CD8^+$ T-cell percentage, 46% (range, 19%–79%); mean $CD4^+$ T cell percentage, 30% (range, 2%–54%); mean granulocyte percentage, 56% (range, 20%–77%); mean $CD14^+$ monocyte percentage, 8.10% (range, 4%–24%).

Data Set 7: Whole-Blood Specimens From Controls in GSE42861

Here, we only used the 335 control samples from the report by Liu et al [37] (ie, from subjects without rheumatoid arthritis). The cell proportions for each control were estimated by Dr Yun Liu [37], using the Houseman method [38].

Data Set 8: Sorted Leukocytes From Individuals in GSE39981

The authors isolated PMBCs by magnetic-activated cell sorting (Miltenyi Biotec) and confirmed purity by fluorescence-activate cell sorting [39]. We focused here on data from 4 individuals for whom complete data on monocytes, neutrophils, B cells, pan T

cells, $CD4^+$ T cells, natural killer (NK) cells, and granulocytes were available.

Data Set 9: Blood Cell Type Data From Healthy Males in GSE35069

The authors analyzed sorted blood cells ($CD4^+$ T cells, $CD8^+$ T cells, $CD56^+$ NK cells, $CD19^+$ B cells, $CD14^+$ monocytes, neutrophils, and eosinophils) from 6 healthy male blood donors with a mean age (±SD) of 38 ± 13.6 years [40].

Data Set 10: $CD4^+$ T cells and $CD14^+$ Monocytes From Healthy Subjects in GSE20242

The authors used the Illumina Infinium 27 K array to analyze $CD4^+$ T cells and $CD14^+$ monocytes from the same individuals [16]. We restricted the analysis to the 23 healthy subjects for whom both cell types were available.

Data Set 11: Sorted Blood Cells From 6 Healthy Volunteers in E–ERAD–179

The authors measured DNA methylation levels from whole PBMCs and cell subsets (CD4, CD8, CD14, CD19, and CD16) from 6 healthy volunteers [41].

DNA Methylation Age and the Epigenetic Clock

The epigenetic clock is defined as a prediction method of age, based on the linear combination of the DNA methylation levels of 353 CpG dinucleotides [25]. Predicted age, referred to as DNA methylation age, correlates with chronological age in sorted cell types ($CD4^+$ T cells, monocytes, B cells, glial cells, and neurons) and tissues and organs, including whole blood, brain, breast, kidney, liver, lung, and saliva [25]. By construction, the epigenetic clock (and software) applies to data generated using either the Illumina 450 K or 27 K platform. Mathematical details and software tutorials for the epigenetic clock can be found in the additional files of the article by Horvath [25]. An online age calculator can be found at our website (available at: http://labs.genetics.ucla.edu/horvath/dnamage/).

Blood Cell Count Estimates

Flow cytometry measures of blood cell counts were assessed by the Multicenter AIDS Cohort Study in Los Angeles as described previously [42]. For data sets involving controls (eg, data set 7), blood cell proportions ($CD8^+$ T cells, $CD4^+$ T cells, NK cells, B cells, and granulocytes) were estimated using Houseman's estimation method [38], which is based on DNA methylation signatures from purified leukocyte samples. The percentage of exhausted $CD8^+$ T cells (defined as $CD28^-CD45RA^-$ B cells) and the number of naive CD8+ T cells (defined as $CD45RA^+CCR7^+$ B cells) were estimated using the advanced analysis option of the epigenetic clock software [25].

RESULTS

Brain Tissue Specimens From Cases and Controls

Using the first brain data set, we observed a strong correlation between DNA methylation age and chronological age in all brain regions (Figure 1*A*–*D*). Regression lines through samples from cases only (Figure 1*A*–*C*) and controls only (black lines) suggest that cases have a DNA methylation age that is older than that of controls.

To perform a formal statistical analysis, we defined a measure of epigenetic age acceleration as the difference between the observed DNA methylation age value and that predicted by a linear model in controls. A positive value indicates that the DNA methylation age is higher than that predicted from the linear model for controls of the same age. On average, brain samples from cases exhibited significant age acceleration effects ($P = 8.0 \times 10^{-8}$; Figure 1*E*), but these effects depended on brain region: significant age acceleration effects were observed in the occipital cortex ($P = 9.6 \times 10^{-5}$; Figure 1*F*) and the cerebellum ($P = .036$; Figure 1*G*) but not in the frontal lobe (Figure 1*H*). We caution that differences in age acceleration effects may reflect low sample sizes or technical variability. But the difference between the cerebellum and frontal lobe was reproducible in independent data sets. Using brain data set 3, we observed again a significant age acceleration effect in the cerebellum ($P = .031$ [Figure 2*C*]; 7.4 years [Supplementary 1]). But we did not observe an accelerated aging effect in the second frontal lobe data set (data set 2; Figure 2*D*), which is congruent with our findings in data set 1 (Figure 1*H*). Future research will need to clarify why HIV infection seems to accelerate the age of some brain regions (eg, the occipital lobe and cerebellum) but not that of others (eg, the frontal lobe). To estimate the effect of age acceleration in terms of years, we used a linear regression model that regressed DNA methylation age on chronological age and viral load status (Supplementary 1). The analysis suggested that brain regions of cases were, on average, 7.4 years older than those of controls. The estimated acceleration effect was 9.3 years in the occipital cortex, 5 years in the cerebellum, and 0.1 years in the frontal lobe.

Overall, HIV load in the CSF of cases was not significantly correlated with age acceleration in the brain samples (Figure 1*I*–*K*), but there was a marginally significant effect in the frontal lobe ($r = 0.42$, $P = .065$; Figure 1*L*). Since viral load was not ascertained in brain tissue, we could not correlate it with epigenetic age acceleration in the respective brain regions.

More-detailed examination is required to determine the cellular and histopathological correlates of age acceleration in HIV-infected brains. Table 2 provides clinical information about the cases from whom autopsy brain samples were analyzed. Unfortunately, cause of death is not collected by the NNTC, although these data are often unreliable because of the multiple comorbidities of the participants. However, and

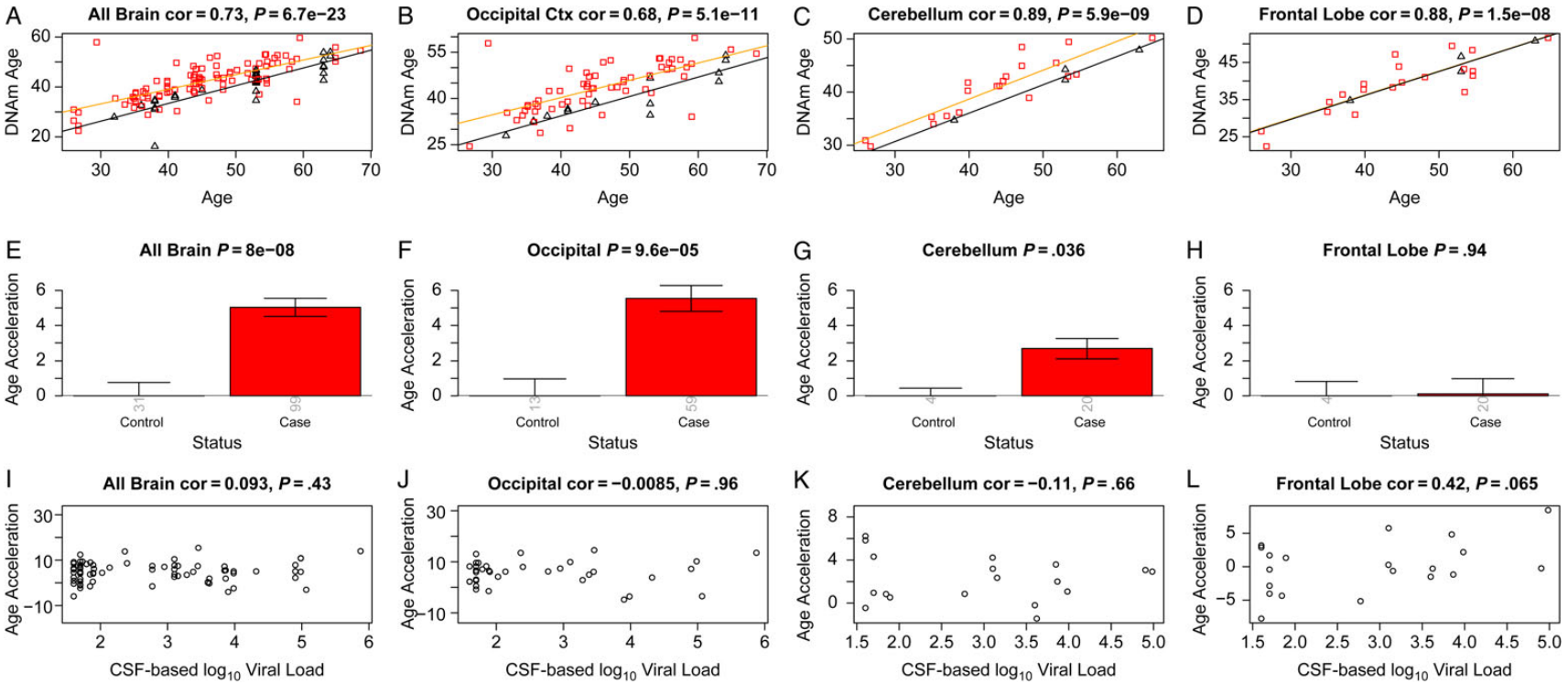

Figure 1. Discovery brain data from human immunodeficiency virus (HIV)–infected subjects (cases) and HIV-uninfected subjects (controls). *A–D*, DNA methylation (DNAm) age versus chronological age in all brain samples (*A*) and occipital cortex (*B*), cerebellum (*C*), and frontal lobe (*D*) samples. Red squares and black triangles in the scatterplot denote samples from cases and controls, respectively. The orange line depicts a linear regression line through case samples. Similarly, the black solid line corresponds to a regression line of DNAm age on chronological age in control samples. For each subject (point), age acceleration is defined as the vertical distance to the black regression line (ie, DNAm age minus the expected value based on control samples). *E*, Mean age acceleration versus control status in all brain samples. Each bar plot depicts 1 standard error around the mean value and reports the Kruskal–Wallis (nonparametric) group comparison test *P* value. Analogous results can be obtained when restricting the analysis to occipital cortex (*B* and *F*) or cerebellar (*C* and *G*) samples but not for samples from the frontal lobe (*D* and *G*). *E–H*, The group comparisons in panels *E–H* involved a total of 130, 72, 24, and 24, samples respectively. The number of samples in each group is reported by the rotated number under each bar. *I–L*, HIV load (log_{10} transformed) in cerebrospinal fluid (CSF) of cases versus age acceleration in all brain samples (*I*) and occipital cortex (*J*), cerebellum (*K*), and frontal lobe (*L*) samples. Abbreviation: cor, correlation.

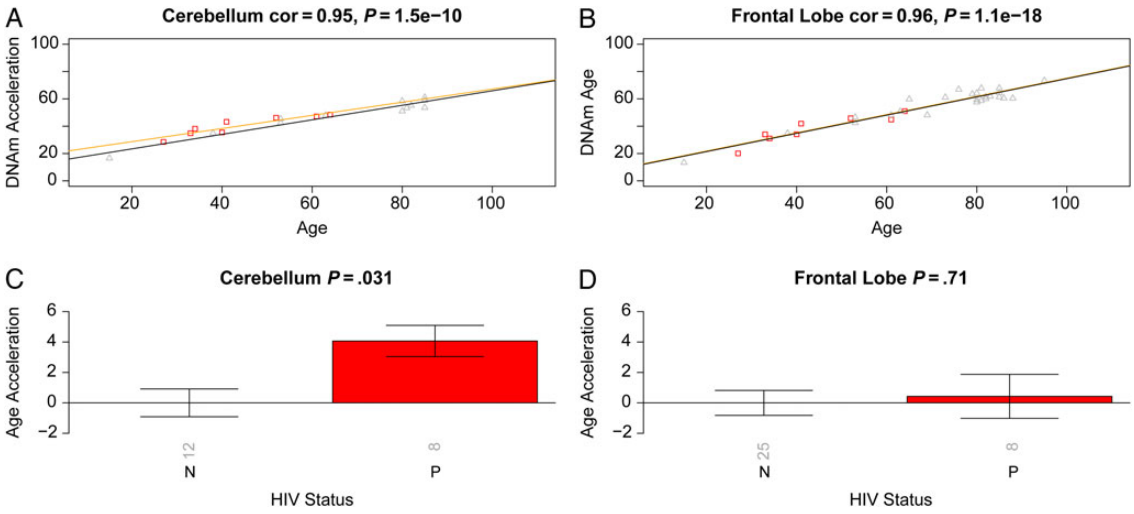

Figure 2. Validation brain data from human immunodeficiency virus (HIV)–infected subjects (cases) and HIV-uninfected subjects (controls). Analogous to Figure 1, we used independent data sets (data 2 and 3) to relate HIV status to epigenetic age acceleration in the frontal lobe and cerebellum of cases and controls. *A* and *B*, DNA methylation (DNAm) age versus chronological age in cerebellum (*A*) and frontal lobe (*B*) samples. Points (subjects) are colored by HIV status: cases correspond to red squares. The orange and black lines depict regression lines case and control samples, respectively. The measure of age acceleration is the same as used in Figure 1. *C* and *D*, Age acceleration versus HIV status in cerebellum (*C*) and frontal lobe (*D*) specimens. Each bar plot reports the Kruskal–Wallis (nonparametric) group comparison test *P* value and 1 standard error around the mean. Abbreviation: cor, correlation.

more relevant, considering that we examined brain DNA, the NNTC conducts neuropathological examination according to a standard protocol. While the brain pathologies from HIV-infected individuals do not necessarily translate to specific diseases or clinical syndromes and are not uncommon in individuals with advanced HIV infection, these data indicated that, of the 31 cases with noted brain pathology, several had >1 type. All cases received a diagnosis ≤1 year prior to death indicating that they were neurocognitively normal or had an HIV-associated neurocognitive disorder (as reported elsewhere [33]). We also included in Table 2 virologic and clinical variables. Note that in some instances this information was not collected. According to the autopsy results, 8 cases had HIV-associated encephalitis. Greater number of perivascular macrophages are found in the brains of patients with HIV encephalitis [43]. While we cannot rule out that the observed age acceleration effects reflect changes in cellular composition (eg, increased numbers of perivascular macrophages), we could not find a significant relationship between epigenetic age acceleration effects in brain samples from cases and a marker of activated macrophages, namely ionized calcium-binding adapter molecule 1 (IBA1), which is encoded by the gene allograft inflammatory factor 1. The IBA1 marker was assessed using immunohistochemical staining of paraffin embedded tissue, as described in "Methods" section.

Blood Specimens From Cases and Controls

Using 2 independent blood data sets, we observed that cases exhibited a significant age acceleration effect ($P = .0048$ [Figure 3*C*] and $P = .00036$ [Figure 3*D*]). A linear model analysis revealed that the DNA methylation age of cases was, on average, 5.2 years greater than that of controls (3.7 years in blood data set 4 and 6.7 years in blood data set 5; Supplementary 1). Since we analyzed whole blood (as opposed to sorted blood cells), we cannot rule out that the observed epigenetic age acceleration effects were mediated by changes in blood cell composition.

Epigenetic Age Acceleration Versus Blood Cell Counts in Adult Male Cases

We used PBMCs from 109 adult male cases (data set 6) to study the relationship between epigenetic age, HIV load, and blood cell counts. DNA methylation age was closely related with chronological age in these cases ($r = 0.80$; median error, 3.9 years; Figure 4*A*). We defined a measure of epigenetic age acceleration as the residual from a linear regression line (Figure 4*A*). A multivariate regression analysis suggested that cases with detectable viral load (ie, >35 copies/mL) had a DNA methylation age that was on average 3.6 years greater than that of adult male cases with a nondetectable viral load, but the association was only marginally significant ($P = .033$) and requires further validation studies. About 92% of cases were receiving antiretroviral therapy, but we were unable to assess who was adherent to their medications. Thus, detectable viral load could be due to a lack of adherence or to treatment failure. Epigenetic age acceleration correlated with several cell count measures in these cases, including NK cells ($r = 0.33$, $P = 4 \times 10^{-4}$; Figure 4*B*), monocytes ($r = 0.2$, $P = .05$; Figure 4*C*), granulocytes ($r = -0.37$, $P = .00019$; Figure 4*D*), $CD4^+$ T cells ($r = -0.23$, $P = .023$; Figure 4*E*), $CD8^+$ T cells ($r = 0.24$, $P = .017$; Figure 4*F*), exhausted ($CD28^-CD45RA^-$)

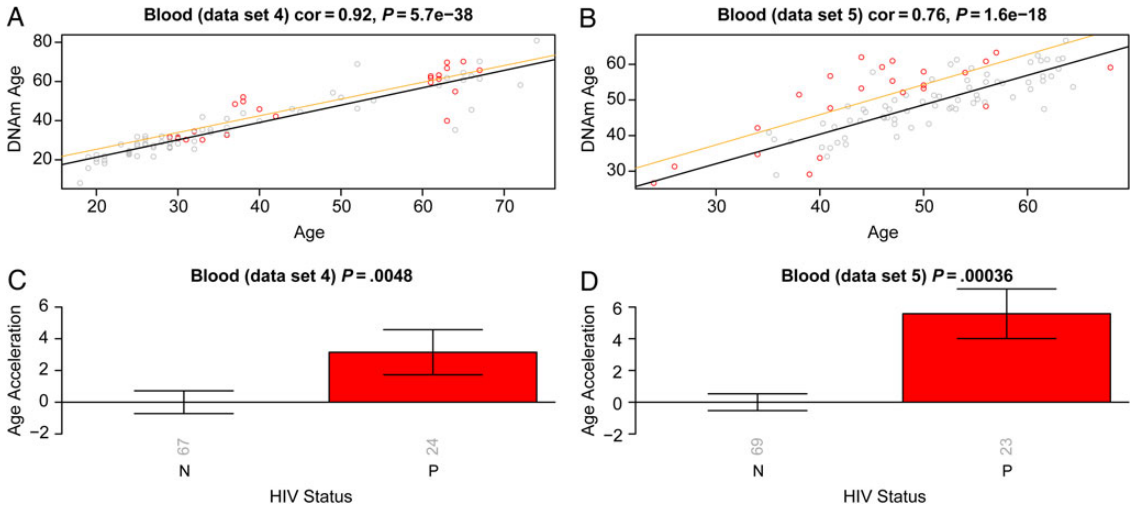

Figure 3. Epigenetic age in blood tissue versus human immunodeficiency virus (HIV) status. The first column (*A* and *C*) and second column (*B* and *D*) report findings for blood data sets 4 and 5, respectively. *A* and *B*, DNA methylation (DNAm) age versus chronological age. Samples from HIV-infected patients (cases; points) are colored in red. The black solid line and the orange line correspond to regression lines through HIV-uninfected control samples and case samples, respectively. For each subject (point), age acceleration is defined as the vertical distance to the black regression line. *C* and *D*, Mean age acceleration versus HIV status. The rotated numbers on the *x*-axis report the group sizes. The bar graphs report 1 standard error and a Kruskal–Wallis test *P* value. Abbreviation: cor, correlation.

$CD8^+$ T cells ($r = 0.36$, $P = 1.0 \times 10^{-4}$; Figure 4*H*), and the number of naive ($CD45RA^+CCR7^+$) $CD8^+$ T cells ($r = -0.26$, $P = .0059$; Figure 4*G*).

Epigenetic Age Acceleration Versus Blood Cell Counts in Controls

In contrast to our findings for cases, epigenetic age acceleration exhibited weaker correlations with blood cell count measures in controls (Figure 5). The highest correlation was observed for the percentage of exhausted $CD8^+$ T cells in the controls from blood data set 5 ($r = 0.29$, $P = .016$; Figure 5*H*), but this finding was not validated in an independent data set (data set 7; Figure 5*P*). These findings are congruent with the fact that sorted blood cells appear to have similar DNA methylation ages (Supplementary 2). The relatively small sample sizes provided by data sets 8–11 did not provide sufficient statistical power for detecting significant differences in DNA methylation age between blood cells (B cells, $CD4^+$ T cells, $CD8^+$ T cells, eosinophils, granulocytes, monocytes, NK cells, and neutrophils) isolated from the same controls (Supplementary 2).

DISCUSSION

In the following, we discuss several models that could explain the relationship between HIV status and epigenetic age acceleration.

Model 1 assumes that changes in telomere length mediate the effect of HIV infection on epigenetic age acceleration (ie, HIV infection → telomere length → epigenetic age acceleration). This model is probably incorrect because (1) there seems to be at best a very weak correlation between leukocyte telomere length and epigenetic age acceleration [44], and (2) it is difficult to adapt this model to explain age acceleration effects in brain tissue.

Model 2 posits that the effect of HIV load on age acceleration is mediated by increases in the amount of senescent or exhausted T cells, such as $CD28^-CD45RA^-$ $CD8^+$ T cells (ie, HIV infection → exhausted/senescent T cells → age acceleration). Our blood data support this model to some extent: we found that the amount of exhausted $CD8^+$ T cells correlated with epigenetic age acceleration in cases (Figure 4*H*) and, to a lesser extent, in controls (Figure 5*H* and 5*P*). But it is difficult to use this model for explaining accelerated aging effects in brain tissue, owing to the blood-brain barrier.

Model 3 is the independent model, in which HIV infection causes increases in exhausted T-cell counts and age acceleration independently (ie, exhausted/senescent T cells ← HIV infection → age acceleration). In other words, HIV infection confounds the relationship between the exhausted T-cell count and age acceleration. This is a plausible model, but it leaves us with the question of how HIV infection leads to epigenetic age acceleration. At this point, it is difficult to address this question since it is unknown what is being measured by DNA methylation age. Several lines of indirect evidence suggest that DNA methylation age might measure the cumulative work done by an epigenomic maintenance system [25]. In support of this hypothesis, HIV-1 infection is known to induce double-strand breaks of chromosomal DNA [45] and to induce chromosomal DNA damage

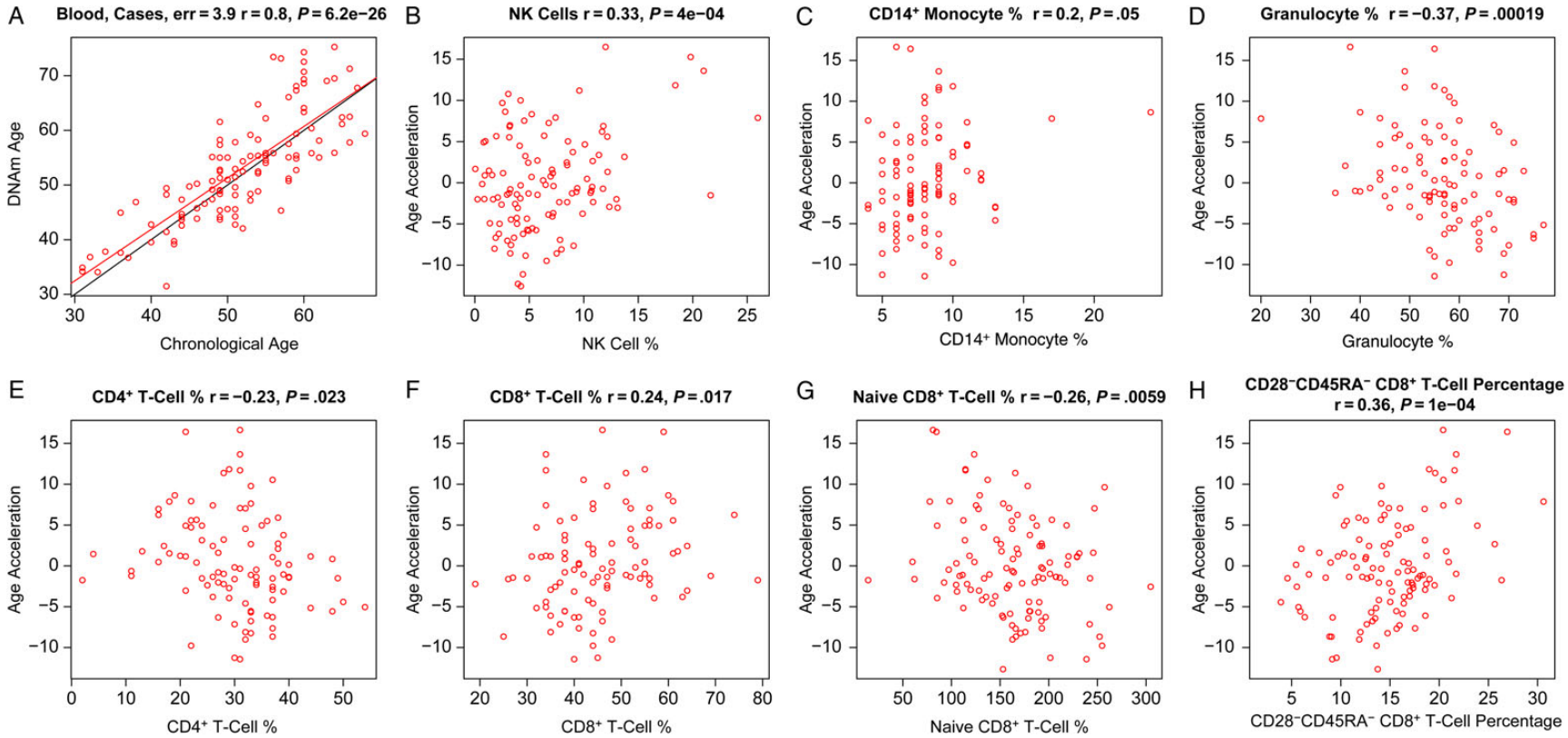

Figure 4. Age acceleration versus blood cell counts in human immunodeficiency virus (HIV)–infected subjects (cases). Here we used DNA methylation (DNAm) data from peripheral blood mononuclear cells from cases (data set 6). *A*, DNAm age versus age. The red line indicates the regression line. The black line corresponds to $y = x$. Epigenetic age acceleration (defined as the residual) versus the percentage of natural killer (NK) cells (*B*), $CD14^+$ monocytes (*C*), granulocytes (*D*), $CD4^+$ T cells (*E*), $CD8^+$ T cells (*F*), naive $CD8^+$ T cells (*G*), and exhausted ($CD28^-CD45RA^-$) $CD8^+$ T cells (*H*).

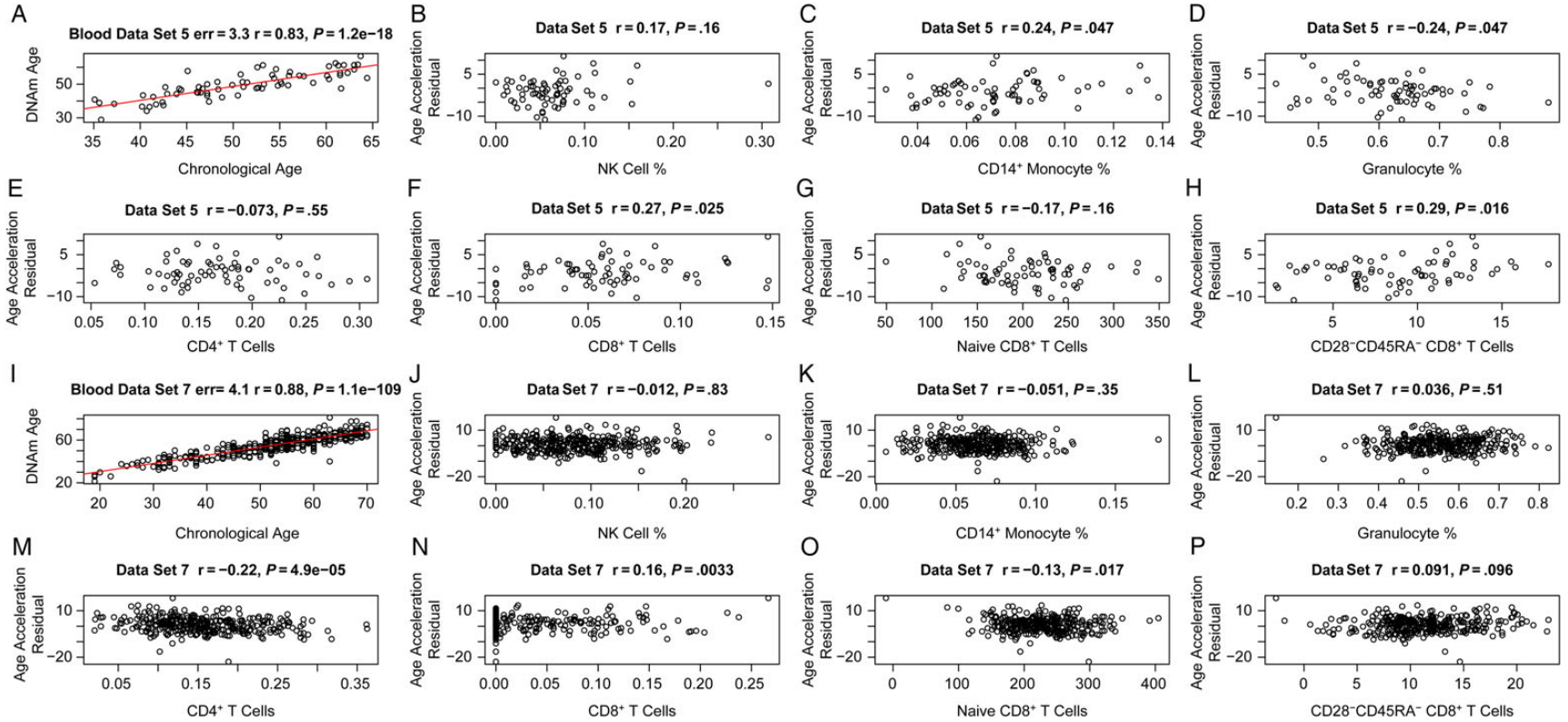

Figure 5. Age acceleration versus blood cell counts in HIV-uninfected control subjects (controls). The first 2 rows (*A*–*H*) and the last 2 rows (*I*–*P*) present results for controls from blood data sets 5 and 7, respectively. *A* and *I*, DNA methylation (DNAm) age versus chronological age. Age acceleration was defined as the residual resulting from the regression line (red line). Age acceleration versus natural killer (NK) cells (*B* and *J*), $CD14^+$ monocytes (*C* and *K*), granulocytes (*D* and *L*), $CD4^+$ T cells (*E* and *M*), $CD8^+$ T cells (*F* and *N*), naive $CD8^+$ T cells (*G* and *O*), and exhausted ($CD28^-CD45RA^-$) $CD8^+$ T cells (*H* and *P*). The blood cell abundance measures were estimated on the basis of DNAm data ("Methods" section).

responses by activating Rad3-related or ataxia-telangiectasia mutated proteins and by promoting phosphorylation of their downstream substrates [46, 47]. If one assumes that viral integration into the host genome leads to epigenomic instability (related to genetic instability), then the observed accelerated aging effects could reflect the protective actions of the epigenomic maintenance system.

Our study has several limitations, including the following. First, we analyzed relatively few controls in our brain data sets (n = 13 in data set 1) because it is difficult to obtain brain samples from relatively young, deceased subjects. Second, our observational study may be biased by hidden confounders that distinguish controls from cases. Third, we were not able to assess whether detectable viral load in cases was due to treatment failure or lack of adherence to the treatment. The weak association between age acceleration and viral load may reflect the fact that viral load does not capture the history of viral load burden. Controlled in vitro studies would be helpful for understanding the relationship between viral load and age acceleration.

In conclusion, we demonstrate that HIV infection is associated with a significant increase in DNA methylation age in brain and blood tissue. Our results are consistent with the reported clinical manifestations of accelerated aging effects among HIV-infected adults despite apparent viral control. Future studies will need to explore whether the epigenetic clock can serve as a useful tool for the study of and/or inform therapeutic strategies aimed at preventing HIV-associated non–AIDS-defining conditions such as cardiovascular disease and HIV-associated neurocognitive disorder [6, 48].

Supplementary Data

Supplementary materials are available at *The Journal of Infectious Diseases* online (http://jid.oxfordjournals.org). Supplementary materials consist of data provided by the author that are published to benefit the reader. The posted materials are not copyedited. The contents of all supplementary data are the sole responsibility of the authors. Questions or messages regarding errors should be addressed to the author.

Notes

Acknowledgments. S. H. conceived of the study and performed the statistical analysis. S. H. and A. J. L. wrote the article. A. J. L. provided the blood and brain data and assisted with the clinical interpretation.

Financial support. This work was supported by the National Institute on Aging, National Institutes of Health (NIH; grant 5R01AG042511-02 to S. H.); the University of California, Los Angeles (UCLA) AIDS Institute; the UCLA Center for AIDS Research (AI28697); the UCLA Clinical and Translational Science Institute; the National Center for Research Resources; the National Center for Advancing Translational Sciences (UL1TR000124); the National Institute for Drug Abuse, NIH (grant R01DA030913 to A. J. L. and S. H.); the National Institute of Allergy and Infectious Diseases, NIH (grant U01-AI-35040 to the Los Angeles site of the Multicenter AIDS Cohort Study [Roger Detels, principal investigator, UCLA]); and the National NeuroAIDS Tissue Consortium, which consists of the National Neurological AIDS Bank (U01-MH08021 and R24-NS38841; Singer), the Texas NeuroAIDS Research Center (U01-MH083507 and R24-NS45491; Benjamin Gelman, principal investigator, University of Texas Medical Branch), the Manhattan HIV Brain Bank (U01-MH083501 and R24-MH59724; Susan Morgello, principal investigator, Mt. Sinai Medical Center), and the California NeuroAIDS Tissue Network (U01-MH083506 and R24-MH59745; David Moore, principal investigator, UCSD).

Potential conflict of interest. Both authors: No reported conflicts.

Both authors have submitted the ICMJE Form for Disclosure of Potential Conflicts of Interest. Conflicts that the editors consider relevant to the content of the manuscript have been disclosed.

References

1. Fausto A, Bongiovanni M, Cicconi P, et al. Potential predictive factors of osteoporosis in HIV-positive subjects. Bone **2006**; 38:893–7.
2. Triant VA, Lee H, Hadigan C, Grinspoon SK. Increased acute myocardial infarction rates and cardiovascular risk factors among patients with human immunodeficiency virus disease. J Clin Endocrinol Metab **2007**; 92:2506–12.
3. Lucas GM, Mehta SH, Atta MG, et al. End-stage renal disease and chronic kidney disease in a cohort of African-American HIV-infected and at-risk HIV-seronegative participants followed between 1988 and 2004. AIDS **2007**; 21:2435–43.
4. Silverberg M, Chao C, Leyden W, et al. HIV infection and the risk of cancers with and without a known infectious cause. AIDS **2009**; 23:2337–45.
5. Martin J, Volberding P. HIV and premature aging: a field still in its infancy. Ann Intern Med **2010**; 153:477–9.
6. Deeks SG. HIV infection, inflammation, immunosenescence, and aging. Annu Rev Med **2011**; 62:141–55.
7. Desquilbet L, Jacobson LP, Fried LP, et al. A frailty-related phenotype before HAART initiation as an independent risk factor for AIDS or death after HAART among HIV-infected men. J Gerontol A Biol Sci Med Sci **2011**; 66A:1030–8.
8. Silverberg MJ, Chao C, Leyden WA, et al. HIV infection, immunodeficiency, viral replication, and the risk of cancer. Cancer Epidemiol Biomarkers Prev **2011**; 20:2551–9.
9. Womack JA, Goulet JL, Gibert C, et al. Increased risk of fragility fractures among HIV infected compared to uninfected male veterans. PLoS One **2011**; 6:e17217.
10. Wendelken L, Valcour V. Impact of HIV and aging on neuropsychological function. J Neurovirol **2012**; 18:256–63.
11. Kirk GD, Mehta SH, Astemborski J, et al. HIV, age, and the severity of hepatitis C virus–related liver disease A cohort study. Ann Intern Med **2013**; 158:658–66.
12. Greene M, Justice A, Lampiris H, Valcour V. Management of human immunodeficiency virus infection in advanced age. JAMA **2013**; 309:1397–405.
13. High KP, Brennan-Ing M, Clifford DB, et al. HIV and aging: state of knowledge and areas of critical need for research. A report to the NIH Office of AIDS Research by the HIV and Aging Working Group. J Acquir Immune Defic Syndr **2012**; 60(Suppl 1):S1–18.
14. Christensen B, Houseman E, Marsit C, et al. Aging and environmental exposures alter tissue-specific DNA methylation dependent upon CpG Island context. PLoS Genet **2009**; 5:e1000602.
15. Bollati V, Schwartz J, Wright R, et al. Decline in genomic DNA methylation through aging in a cohort of elderly subjects. Mech Ageing Dev **2009**; 130:234–9.
16. Rakyan VK, Down TA, Maslau S, et al. Human aging-associated DNA hypermethylation occurs preferentially at bivalent chromatin domains. Genome Res **2010**; 20:434–9.
17. Teschendorff AE, Menon U, Gentry-Maharaj A, et al. Age-dependent DNA methylation of genes that are suppressed in stem cells is a hallmark of cancer. Genome Res **2010**; 20:440–6.
18. Vivithanaporn P, Heo G, Gamble J, et al. Neurologic disease burden in treated HIV/AIDS predicts survival. Neurology **2010**; 75:1150–8.
19. Horvath S, Zhang Y, Langfelder P, et al. Aging effects on DNA methylation modules in human brain and blood tissue. Genome Biol **2012**; 13:R97.

20. Numata S, Ye T, Hyde TM, et al. DNA methylation signatures in development and aging of the human prefrontal cortex. Am J Hum Genet **2012**; 90:260–72.
21. Alisch RS, Barwick BG, Chopra P, et al. Age-associated DNA methylation in pediatric populations. Genome Res **2012**; 22:623–32.
22. Johansson A, Enroth S, Gyllensten U. Continuous aging of the human DNA methylome throughout the human lifespan. PLoS One **2013**; 8: e67378.
23. Day K, Waite L, Thalacker-Mercer A, et al. Differential DNA methylation with age displays both common and dynamic features across human tissues that are influenced by CpG landscape. Genome Biol **2013**; 14:R102.
24. Bocklandt S, Lin W, Sehl ME, et al. Epigenetic predictor of age. PLoS One **2011**; 6:e14821.
25. Horvath S. DNA methylation age of human tissues and cell types. Genome Biol **2013**; 14:R115.
26. Boks MP, Derks EM, Weisenberger DJ, et al. The relationship of DNA methylation with age, gender and genotype in twins and healthy controls. PLoS One **2009**; 4:e6767.
27. Horvath S, Erhart W, Brosch M, et al. Obesity accelerates epigenetic aging of human liver. Proc Natl Acad Sci U S A **2014**; 111:15538–43.
28. Marioni R, Shah S, McRae A, et al. DNA methylation age of blood predicts all-cause mortality in later life. Genome Biol **2015**; 16:25.
29. Marioni RE, Shah S, McRae AF, et al. The epigenetic clock is correlated with physical and cognitive fitness in the Lothian Birth Cohort 1936. Int J Epidemiol **2015**; pii:dyu277.
30. Horvath S, Garagnani P, Bacalini M, et al. Accelerated epigenetic aging in down syndrome. Aging Cell **2015**; 14:491–5.
31. Morgello S, Gelman B, Kozlowski P, et al. The National NeuroAIDS Tissue Consortium: a new paradigm in brain banking with an emphasis on infectious disease. Neuropathol Appl Neurobiol **2001**; 27:326–35.
32. Heaton R, Kirson D, Velin R, Grant I, Martin A. The utility of clinical ratings for detecting cognitive change in HIV infection. New York: Oxford University Press, **1994** (Grant I, Martin A, eds. Neuropsychology of HIV infection).
33. Dana Consortium. Clinical confirmation of the American Academy of Neurology algorithm for HIV-1-associated cognitive/motor disorder. The Dana Consortium on Therapy for HIV Dementia and Related Cognitive Disorders. Neurology **1996**; 47:1247–53.
34. Antinori A, Arendt G, Becker JT, et al. Updated research nosology for HIV-associated neurocognitive disorders. Neurology **2007**; 69: 1789–99.
35. Soontornniyomkij V, Soontornniyomkij B, Moore DJ, et al. Antioxidant sestrin-2 redistribution to neuronal soma in human immunodeficiency virus-associated neurocognitive disorders. J Neuroimmune Pharmacol **2012**; 7:579–90.
36. Soontornniyomkij V, Risbrough VB, Young JW, et al. Short-term recognition memory impairment is associated with decreased expression of FK506 binding protein 51 in the aged mouse brain. Age (Dordr) **2010**; 32:309–22.
37. Liu Y, Aryee MJ, Padyukov L, et al. Epigenome-wide association data implicate DNA methylation as an intermediary of genetic risk in rheumatoid arthritis. Nat Biotech **2013**; 31:142–7.
38. Houseman E, Accomando W, Koestler D, et al. DNA methylation arrays as surrogate measures of cell mixture distribution. BMC Bioinformatics **2012**; 13:86.
39. Accomando WP, Wiencke JK, Houseman EA, et al. Decreased NK cells in patients with head and neck cancer determined in archival DNA. Clin Cancer Res **2012**; 18:6147–54.
40. Reinius LE, Acevedo N, Joerink M, et al. Differential DNA methylation in purified human blood cells: implications for cell lineage and studies on disease susceptibility. PLoS One **2012**; 7:e41361.
41. Zilbauer M, Rayner TF, Clark C, et al. Genome-wide methylation analyses of primary human leukocyte subsets identifies functionally important cell-type-specific hypomethylated regions. Blood **2013**; 122:e52–60.
42. Ibarrondo FJ, Yang OO, Chodon T, et al. Natural killer T cells in advanced melanoma patients treated with tremelimumab. PLoS One **2013**; 8:e76829.
43. Levine AJ, Panos SE, Horvath S. Genetic, transcriptomic, and epigenetic studies of HIV-associated neurocognitive disorder. J Acquir Immune Defic Syndr **2014**; 65:481–503.
44. Boks MP, Mierlo HCV, Rutten BPF, et al. Longitudinal changes of telomere length and epigenetic age related to traumatic stress and post-traumatic stress disorder. Psychoneuroendocrinology **2015**; 51:506–12.
45. Tachiwana H, Shimura M, Nakai-Murakami C, et al. HIV-1 Vpr induces DNA double-strand breaks. Cancer Res **2006**; 66:627–31.
46. Lau A, Swinbank KM, Ahmed PS, et al. Suppression of HIV-1 infection by a small molecule inhibitor of the ATM kinase. Nat Cell Biol **2005**; 7:493–500.
47. Zimmerman ES, Chen J, Andersen JL, et al. Human immunodeficiency virus type 1 Vpr-mediated G2 arrest requires rad17 and Hus1 and induces nuclear BRCA1 and γ-H2AX focus formation. Mol Cell Biol **2004**; 24:9286–94.
48. Nath AA. HIV and aging. J Neurovirol **2012**; 18:245–6.